Original Research Article

Evaluation of the Anti-Microbial Activity of Zero valent iron nanoparticle synthesized using *Aspillia plorizeta* extracts

ABSTRACT

Antimicrobial resistance poses a great burden to existing health care system as more potent drugs are required to combat this global problem. As such there is need to explore new ways in which we can be able to combat antimicrobial resistance hence the need to utilize the potential of metallic nanoparticles as a new alternative to combat resistance. The present study focuses on synthesis of iron nanoparticles using *Aspillia plorizeta* aqueous extracts its characterization and antimicrobial activities against gram positive and gram negative bacteria. Preliminary phytochemical screening was carried out to test for the presence of secondary metabolites; phenol, flavonoid, phytosterol, carbohydrate, tannin, saponin, glycoside and terpenoid resulting in a positive test for all the metabolites. Folin-Ciocalteu method and aluminium chloride method respectively were used in determination of total phenolic content 31.45 ±0.017 mg/g and total flavonoid content 7.223 ±0.081 mg/g. Characterization of zero valent iron oxide NPs was achieved using UV-visible spectrophotometer, FT-IR, XRD and XRF. UV-Vis spectrophotometer displayed a peak at 346 nm. FT-IR spectra portrayed existence of functional groups such as OH, C-O and C-C that aid in formation of NPs. XRD indicated the presence of peaks of peaks at 16.06° and 43.73°.XRF data showed the NPs containing Fe 31.58%, MgO 12.02%, Al_2O_3 1.883%, SiO_2 13.84%, P_2O_5 11.14%, K_2O 4.699% and CaO 1.522% of respective oxides. Thus presence of secondary metabolites in the plant extracts are responsible for the synthesis of iron nanoparticles. Finally the antimicrobial activity was determined against *Staphylococcus aureus*, *Bacillus subtilis*, *Pseudomonas aeruginosa*, *Escherichia coli* and *Candida albicans* which exhibited significant zones of inhibition.

Keywords: Aspillia plorizeta; NPs; Environmental friendly; Characterization; XRF

1. INTRODUCTION

Infectious diseases are the world's leading cause of premature deaths, killing almost 50,000 people every day and with continuous use of antibiotics, microorganism have become resistant (Alavijeh, *et al.,* 2012).Many developing countries more so in Africa, mortality and morbidity rates as a result of diarrhea, which continues to be a major challenge especially amongst children (Hills, *et al*., 2014). Of late drug resistance to human pathogenic bacteria has been commonly reported (Frieri,*et al.*, 2017). In addition to this problem, antibiotics are sometimes associated with adverse effects on host which include hypersensitivity, immunosuppressant and allergic reactions. This has brought immense clinical problems in the treatment of infectious diseases (Alavijeh *et al*., 2012).

According to 2008 study of antibiotic development involving small firms as well as large pharmaceutical companies revealed that only 15 of 167 antibiotics under development had a new mechanism of action (Leung *et al.,* 2011). If the current trend continues, before long there may not be effective antimicrobials with which to treat patients with serious infections.

Nanotechnology which is a modern field of science dealing in production, manipulation and use of very small particles with sizes measured in nanometers has found its application in the field of medicine (Heera & Shanmugam, 2015). Nanoparticles are majorly obtained using chemical and physical process. Production of NPs using plant materials results to low cost of production, short production time, it is relatively safer and its ability to up production. On industrial scale efficient extraction, isolation and purification is a challenge. Plant materials have varying concentration of bio-active components. Size and morphology depends on localization in plant material that depends on differences in content of metal tissues (Makarov, *et al*., 2014) .Various research work has been done using different metal NPs contributing toward the development and synthesis of alternative antimicrobial agents, nano-therapeutics, to treat infections caused by clinical multidrug-resistant strains (Enrique, *et al.,* 2018). Due to their various physiochemical properties such as large surface area, mechanical strength, optical activity and their reactiveness(Khan, *et al.,* 2017), iron nanoparticles has also found application in water treatment (Devatha, *et al*., 2018). Borohydrate reduction of Fe (III) ions in aqueous media to zero valent ions is usually carried out in inert conditions to keep iron in its zero valent form which is unstable in atmospheric conditions and it tends to form oxides/hydroxides in the forms of Fe_3O_4, Fe_2O_3 and FeOOH (Yuvakkumar, *et al.,* 2011).Extraction and isolation of natural products (Xiao, *et al.*, 2018). Biosynthesis have more compensation over other classical synthesis procedures due to availability of more biological entities and eco-friendly procedures it is cost effective, easily scaled up for large scale synthesis ,there is no need to use high pressure, energy, temperature and toxic chemicals (Kuppusamy, *et al.,* 2016; Ksv, *et al.*, 2017).

The plant crude extract contain active secondary metabolites such as phenolic acids, flavonoids, alkaloids and terpenoids which have been reported to be mainly responsible for the reduction of ionic iron leading to formation of bulk metallic nanoparticles. In the present study, iron nanoparticle were synthesized using a rapid, single step, green biosynthetic method employing aqueous extracts of *Aspillia plorizeta* as a reducing agent (Saranya, 2017).

2. MATERIALS AND METHODS

2.1 Collection of plant material

The fresh plant samples were collected, kept in a labelled polythene bag and taken to the laboratory. Thoroughly washed plant material were then air dried in a shade for four days, thereafter crushed into powder form with an in-house mechanical grinder and stored to await chemical analysis (Ahmed, *et al*., 2016)

2.2 Extraction of *Aspillia plorizeta* using water

With slight changes from work done by (Vélez *et al.*, 2018) ,5g of *Aspillia plorizeta* leaves powder was weighed into a 250 conical flask, thereafter 100ml of distilled water added followed by boiling in a water bath for one hour maintaining the temperature at 80°C. Having obtained the extract, it was then filtered using Whatman no.1filter paper .The filtrate was then kept in the refrigerator ready for analysis (Logeswari, *et al.*, 2015).

2.3 Qualitative screening of secondary metabolites

The following standard protocols were used for qualitative analysis to check for the presence of Carbohydrates, Flavonoids, Phenols, Saponins, Tannins, Terpenoids, Phytosterols and glycosdes (Prabhavathi, *et al.*, 2016,Khalid, *et al*., 2018 and Gupta & Gupta, 2014).

2.4 Quantitative Analysis

2.4.1 Total Phenolic Content

The total phenolic content was determined using Folin-Ciocalteu method with slight changes from work done by (Baba & Malik, 2015). Aliquots of working standard solution was pippeted out into a series of test tubes. 50 µL of phenolic extract of the plant sample was then taken into another series of test tubes. Contents of all the test tubes were topped to 1 mL using distilled water. Another test tube labelled blank with 1 mL of distilled water served as the blank. 0.5 mL of Folin-Ciocalteu reagent (1 N) was then added to each test tube including the blank. All the test tubes were vortexed well and allowed to stand for 5 min at room temperature. 2.5 mL of 5 % sodium carbonate was then added to all the test tubes including the blank. The test tubes were again vortexed and incubated in the dark at room temperature for 40 min. Absorbance of the blue color developed was measured against the reagent blank at 769 nm using UV-vis spectrophotometer. Thereafter, the sample concentration was calculated from the gallic acid standard curve equation and the results expressed as mg gallic acid equivalents per gram of dried weight sample. Experiments were carried out in triplicates and expressed as mean ± standard deviation (Alara, *et al.*, 2017).

2.4.2 Total Flavonoids Content

With slight modifications, total flavonoid content of crude extract was determined using aluminium chloride colorimetric method on the basis of a protocol represented by (Baba & Malik, 2015). In brief aliquots of working standard solution was pippeted into a series of labelled test tubes. 100 µL of sample extract was taken into another series of test tubes. All the test tubes contents were topped up to 1 mL with distilled water. Another test tube marked blanked with 1 mL of distilled water served as the blank. Thereafter 150 µL of 5 % sodium nitrite was added to each test tube including the blank followed by vortexing all the test tubes well and incubating at room temperature for 5 min.150 µL of 10 % aluminum chloride was then added to all the test tubes including the blank. The test tubes were again vortexed and incubated at room temperature for 6 min.2 mL of 4 % sodium hydroxide was then added to all the test tubes. The contents of test tubes were then made up to 5 mL using distilled water followed by vortexing and allowing them to stand for 15 min at room temperature. Absorbance of the pink color developed due to the presence of flavonoids was measured against the reagent blank at

511 nm using UV-vis spectrophotometer. Finally, total flavonoid content was calculated from calibration curve, and results expressed as mg rutin equivalent per g dry weight. Experiments were carried out in triplicates and expressed as mean ± standard deviation (Spiridon, *et al*., 2011).

2.5 Preparation of iron salt and synthesis of zero valent iron oxide nanoparticle

Preparation and synthesis of iron NPs was carried out with slight modification of procedure, from previous work done by (Ksv, *et al.*, 2017). 0.1M $FeCl_3.6H_2O$ solution salt was prepared by adding 2.703g of solid $FeCl_3.6H_2O$ into 100ml of distilled water. The mixture was then shaken for about 5 minutes to obtain a homogenous mixture. Thereafter NPs was prepared by adding 0.1M of the salt to plant sample in the ratio of 2:5 in which a black precipitate was observed indicating presence of NPs (Silveira, *et al*., 2017). Formed nanoparticle was then retrieved from the mixture by centrifuging (350rpm for ten minutes) and washing severally using distilled water and finally dried in an oven for characterization(Fierascu, *et al.*, 2014).

2.6 Characterization of zero valent iron NPs

Functional groups which necessitated development of nanoparticles was characterized using a Shimadzu Fourier Transform Infrared Spectrometer, Model FTS-8000 and analysis run using the KBr pellet technique (Madivoli, *et al.*, 2012). The optical properties of zero valent iron NPs was determined using Perkin Elmer Spectrophotometer and the characteristic peaks detected and the peak values of the UV-vis recorded (Groiss, *et al.,* 2017). The crystallinity phase of the nanoparticles was identified using STOE STADIP P X-ray Powder Diffraction System (STOE & Cie GmbH, Darmstadt, Germany) with slight modifications from work done by (Gondwal, 2018).Elemental composition of prepared powder sample was then determined using X-ray fluorescence spectrometry (Santos, *et al*., 2017).

2.7 Antibacterial Activity

Evaluation of the antimicrobial activities against gram positive(*Staphylococcus aureus* and *Bacillus subtilis*), gram negative (*Pseudomonas aeruginosa* and *Escherichia coli*) and yeast bacteria(*Candida albicans*) for the green-synthesized zero valent iron nanoparticle was carried out using standard disc diffusion assay with slight modifications from work done previously(Mostafa et al., 2017). Bacteria used in analysis was obtained from Botany department, Jomo Kenyatta University of Agriculture and Technology, Juja ,Kenya.20 mL of agar was loaded to sterile petri plates. After solidification, 100 µL of overnight bacterial culture was spread to get bacterial lawn. Briefly the zero valent iron nanoparticles were dissolved in dimethyl sulfoxide (DMSO) and serially diluted in Muller Hinton agar in Petri dishes to obtain final concentration: 10^0, 10^{-1}, 10^{-2}, 10^{-3}, 10^{-4} and 10^{-5} µg/ml. Each experiment was done in triplicates. Discs of 6mm in diameter prepared from Whatman's filter paper number 1 were dipped in DMSO without nanoparticle acted as negative control, while Nitrofurantoin (200 mcg) acted as

positive control. After incubation of the plates for 24 h at 37℃, a clear zone growth of inhibition was recorded and expressed as mean ± SD (Groiss *et al*., 2017,).

3. RESULTS AND DISCUSSION

3.1 Phytochemical screening of *Aspillia plorizeta* leaves extract

The results on the phytochemical screening of water leaf extract of *Aspillia plorizeta* is presented in Table 1 below.

Table 1: Phytochemical constituents of *Aspillia plorizeta*

Secondary metabolite	Water extract
Tannin	+
Phytosterol	+
Carbohydrate	+
Terpenoid	+
Flavonoid	+
Sapponin	+
Phenol	+
Glycoside	+

Key: '+' = Present - = absent

Phytochemical are basically divided into two groups, primary and secondary constituents according to their functions in plant metabolism. Primary constituents comprise common carbohydrate while secondary constituents consists; glycosides, flavonoids, terpenes, terpenoids, saponins, phenols and tannins (Ranjitha & Suganthi, 2017). *Aspillia plorizeta* aqueous extract gave a positive test for phytochemical screening of all the secondary metabolites under study and this is shown in table 1 above. The structure of plant extracts is constituted by different metabolites like terpenoid, phenols, or carbohydrates (Martínez-cabanas, *et al*., 2016). These compounds are directly responsible of the extract capacity to carry out the NPs biosynthesis hence the leaves were boiled with the aim of rupturing and releasing intracellular materials into the solution (Ganesan, 2015).

3.2 Quantitative phytochemical screening

The total phenolic and flavonoid contents determined from standard curves (y= 0.0043x+0.0464, R^2=0.9919) and (y=0.064x+0.0061, R^2=0.9955) respectively is presented in table 2 below.

Table 2: Total phenolic and total flavonoid content

Metabolite	Quantity
Total phenolic content	31.45±0.017 mg GE/g DW
Total flavonoid content	7.223± 0.081 mg RE/g DW

Results shown in Table 2 above are presented as the mean ± standard deviation using the correlation and regression applications in the Microsoft Excel 2013. Polarity of extracting solvent, isolation procedure and compounds present constitutes natural extracts activity. Total phenolic content of aqueous extracts calculated from the calibration curve (y=0.0043x+0.0464, R^2=0.9919), was 31.45±0.017 mg/g gallic acid equivalents/g, and the total flavonoid content calculated from the calibration curve (y=0.064x+0.0061, R^2=0.9955), was 7.223±0.081 mg/g rutin equivalents/g. Flavonoids and phenolic contents are always considered to be major contributors for the antioxidant activity of plant materials (Jing, *et al.*, 2015).Flavonoids belongs to a family of natural polyphenolic compounds that include flavone, flavonol, flavonone, flavanonol, and isoflavone derivatives. Number of hydroxyl groups and structure in flavonoids play an important role in metal-binding activity. Iron chelates have shown to have pro-oxidant potential (Marslin *et al*., 2018).

3.3 Observations and UV-vis analysis of Iron nanoparticle

Figure 1 and Figure 2 shows the UV-Visible spectrum of zero valent iron nanoparticle and iron (iii) chloride solution.

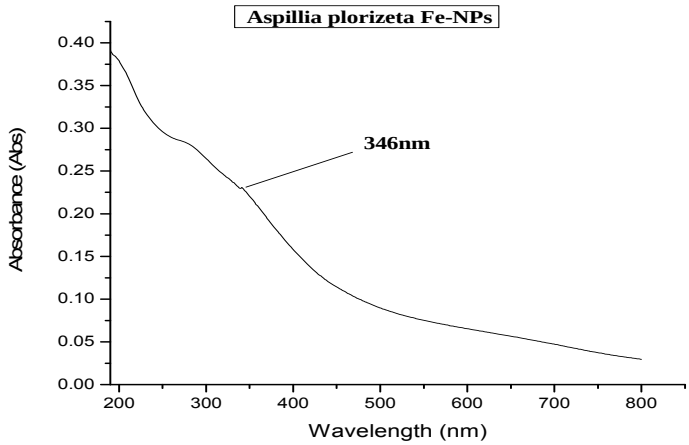

Figure 1: Zero valent iron nanoparticle UV-vis spectrum

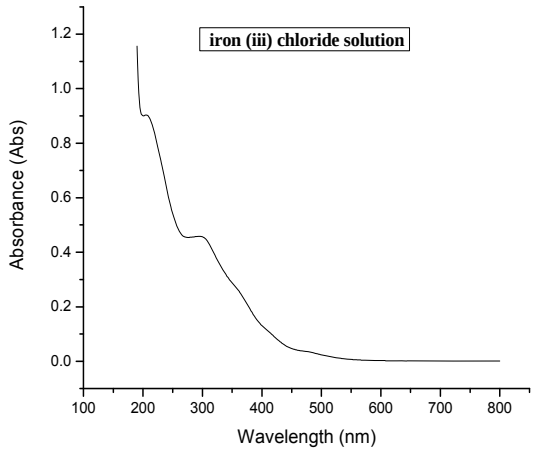

Figure 2: Iron (iii) chloride UV-Vis spectrum

Optical characterization of synthesized zero valent iron nanoparticle was achieved by studying absorption spectra of green synthesized Fe-NPs (fig.1) and aqueous solution of iron (iii) chloride (fig.2).From preliminary characterization of Fe^{3+} ions bio-reduction using UV-Visible absorption spectrum, a peak was recorded at 346nm as shown in (fig.1) which is almost similar from previous work done by (Chaki, *et al.*, 2015). Aqueous solution of iron (iii) chloride gave two peaks at 214nm and 286nm. Thus absence of a peak at 214nm and 286nm in the NPs spectrum could signify formation of zero valent iron NPs. Greater change in absorption spectra, indicates that Aspillia plorizeta alone acts as a better stabilizer, this is in agreement from work done by (Jain & Mehata, 2017) . Presence of a single peak in the NPs developed indicates ,particles formed are of uniform size and shape (Joe, *et al*., 2011).Upon addition of *Aspillia plorizeta* leaf extract into $FeCl_3$ solutions in the ratio of 5:2 at room temperature a visible color change was observed as the yellow aqueous solution of $FeCl_3$ turned to black (Balamurugan, *et al*., 2014). Color change is the most easy and commonly used indicator of metal nanoparticles formation (Atarod, *et al.,* 2016).

3.4 FT-IR characterization

Figure 3 shows the FT-IR spectrum of *Aspillia plorizeta* iron oxide nanoparticle.

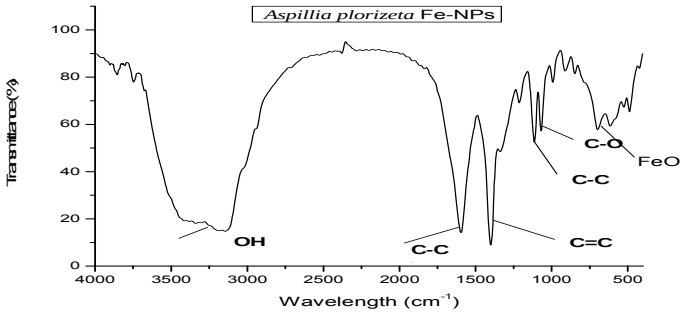

Figure 3: FTIR analysis of Zero Valent Iron nanoparticle

The strong and broad peak at 3145.7cm^{-1} is due to OH stretching vibration arising from hydroxyl groups from the phenolics on nanoparticles, it also denotes reduction of the iron (iii) chloride. The absorption peaks 700.1cm^{-1} and 619.1cm^{-1} corresponds to the Fe-O bond vibration of the formed nanoparticle, absorption peak 1400.2cm^{-1} corresponds to aromatic stretch of C=C while the peak at 1596.9cm^{-1} is attributed to C-C stretch ring in aromatics. Peaks at 1000-1300 cm^{-1} corresponds to C-O stretching vibrations (Khodadadi,*et al.*, 2017). Other remaining peaks corresponds to small amount of organic acids responsible for low pH of the sample helping in synthesis of NPs (Kanagasubbulakshmi*, et al.,* 2017). From the FT-IR analysis in (fig. 3) presence of hydroxyl groups of phenolic in plant extract acts as bio-reductant agents and are directly responsible for reduction of Fe^{3+} ions to zero valent iron NPs (Samaneh, *et al.*, 2017).

3.5 X-Ray Diffraction (XRD)

Figure 4 shows the x-ray powder diffraction patterns for zero valent iron nanoparticles

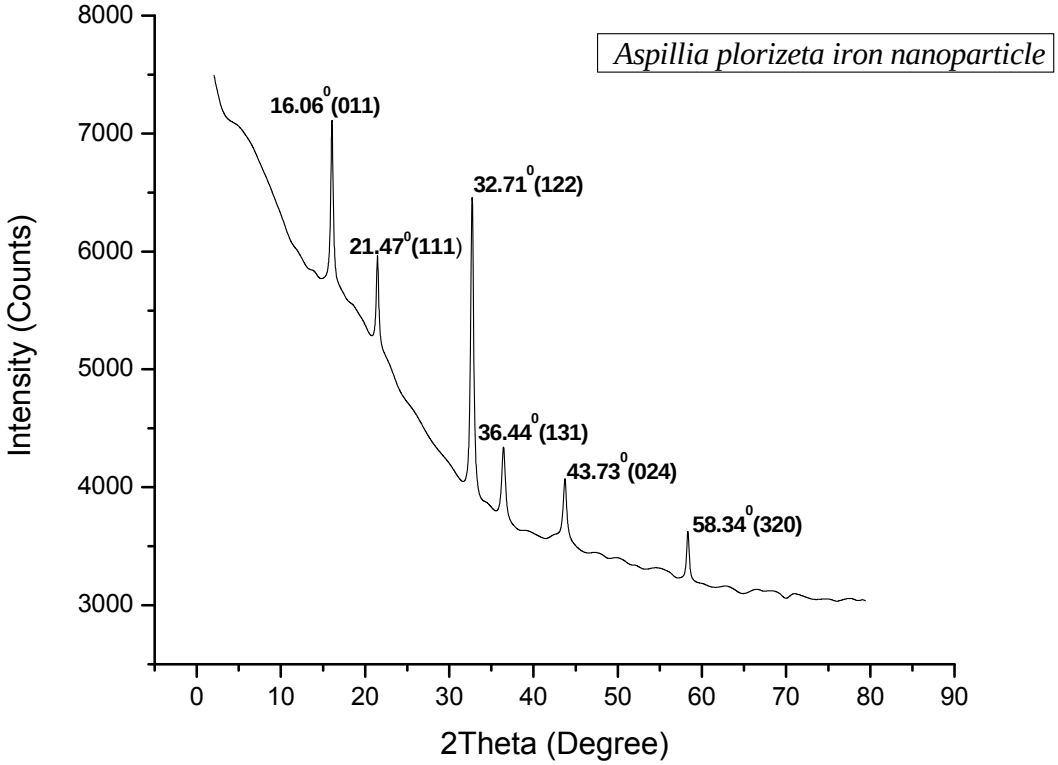

Figure 4: XRD analysis of Zero Valent Iron nanoparticles

Crystallinity of the zero valent iron nanoparticles was determined by analysis of XRD patterns shown in Fig. 4.Characteristic peaks shown by the freshly prepared zero valent iron nanoparticles were 2theta=(16.06°,21.47°,32.71°,36.44°,43.73° and 58.34°).Peak at 16.06° indicates polyphenols present in plant that aids in reduction of iron (iii) salts while peak at 43.73° indicates formation of zero valent iron nanoparticles(Yuvakkumar et al., 2011).Other remaining peaks 21.47° could be as a result of iron oxohydroxide (FeOOH),36.44° is due to presence of magnetite (Groiss et al., 2017) ,32.71° is almost similar to work done by (Jain & Mehata, 2017) and 58.34° was as a result of the bioorganic crystallization on the surface of the nanoparticles(Rafi *et al.*, 2018). Corresponding crystal planes of various peaks shown in fig. 4 above are 011,111,122,131,024 and 320 respectively. Formation of the various crystal planes emanated from crystallite growth of iron metal with oxygen species (Marslin et al., 2018).Presence of distinctive diffraction peaks indicates formed NPs are not amorphous(Wang, Fang, & Megharaj, 2014). From the XRD spectrum it is evident that as intensity increases the peaks also increases this is due to capping of biomaterials from *Aspillia plorizeta* leaf extract on surface of nanoparticles (Ullah, *et al.,* 2018).

3.6 X-Ray Fluorescence Spectrophotometric analysis

XRF spectroscopy was used to determine the elemental composition of the precipitate formed and the results are depicted in figure 5.

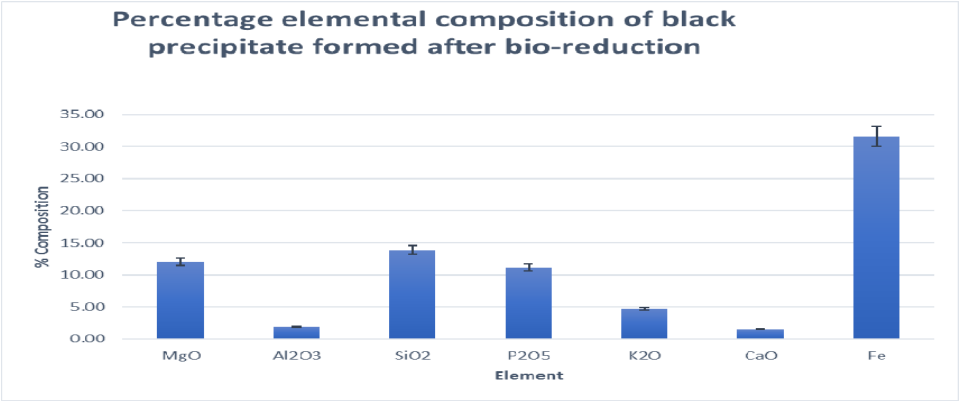

Figure 5: Percentage elemental composition of black precipitate formed after bio-reduction

X-RF spectrophotometer was used to determine elemental composition, results obtained confirmed presence of Fe 31.58%, MgO 12.02%, Al_2O_3 1.883%, SiO_2 13.84%, P_2O_5 11.14%, K_2O 4.699% and CaO 1.522% .Thus from data in (figure. 5) ,presence of iron in developed nanoparticle was confirmed. Relatively higher percentage of FeO was as a result of bio-reduction of Fe^{3+} ions. SiO_2 (13.84%) in the developed nanoparticle provides the following merits; helps in binding various biological or the other ligands at NPs surface for various application, helps nanoparticles to possess good biocompatibility and avoids interparticle interaction.(Wu, He, & Jiang, 2008).

3.7 Antimicrobial activity

Figure. 6 shows the observed zone of inhibition of the five selected microorganisms and various concentrations of developed NPs obtained through serial dilutions.

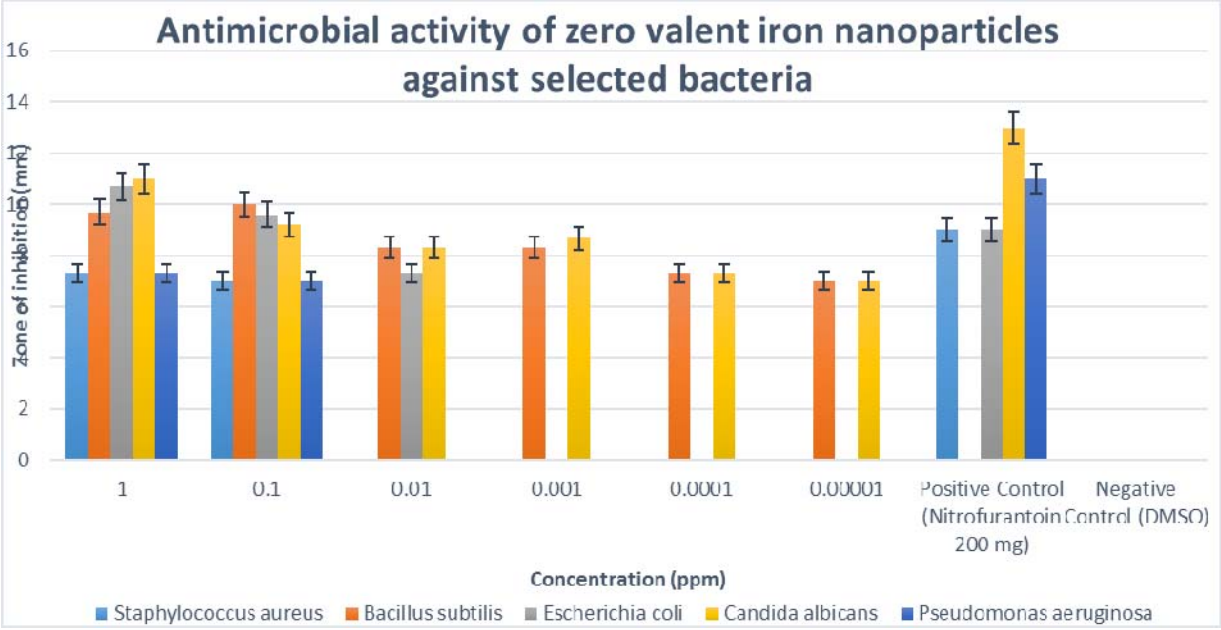

Figure: 6 Antimicrobial activity of zero valent iron nanoparticles against selected bacteria

Antibiotic susceptibility test applied in our present study was the standard disk diffusion assay on the following microorganism *Bacillus subtilis*, *Escherichia coli*, *Pseudomonas aeruginosa*, *Staphylococcus aureus* and *Candida albicans*. The zones of inhibition (mm) exhibited by the various concentrations of synthesized nanoparticle in relation to the standard drug (Nitrofurantoin 200 mg) is presented in figure 6 above. Of the five selected microorganism, the developed NPs is more effective in *Escherichia coli* at concentrations above (0.1ppm) in comparison to the standard drug which had a zone of inhibition (9.000 mm)*. Pseudomonas aeruginosa, Candida albicans* and *Staphylococcus aureus* were the most resistant strains. The negative control in our experiment was (DMSO) did not exhibit any zone of inhibition. *Bacillus subtillis* was more effective at even very lower concentrations(0.00005ppm) Polyphenols are well recognized for their antibacterial activities (Devatha *et al.*, 2018).Polyphenols with iron nanoparticles binding play an important role in prevention of oxidative stress caused by generation of reactive oxygen species. Mechanism of antimicrobial activity of the iron nanoparticle can be summarized in three steps; antibiotic enters the cell, thereafter it must accumulate to a minimum concentration within the cell and finally it acts on its target. The antimicrobial potential of zero valent iron nanoparticles is similar to the original aqueous plant extract (Kanagasubbulakshmi & Kadirvelu, 2017).

CONCLUSION AND RECOMMENDATIONS

Results exhibited from characterization and antimicrobial activity of zero valent iron nanoparticles, is a confirmation that *Aspillia plorizeta* aqueous can be used as a reducing and stabilizing agent in synthesis of nanoparticles .Incorporating green synthesis approach in our studies provides a clean, cheap and safer method. Even though nanoparticles have been used extensively for applications such drug discovery, drug conveyance and disease diagnostics, availability of different plant species which have not been explored, provides scientists with another great opportunity to discover other new therapeutic agents which could act efficiently against target bacteria, thus quelling the challenge of drug resistance.

REFERENCES

Ahmed, S., Saifullah, Ahmad, M., Swami, B. L., & Ikram, S. (2016). Green synthesis of silver nanoparticles using Azadirachta indica aqueous leaf extract. *Journal of Radiation Research and Applied Sciences*, *9*(1), 1–7.

Alara, O. R., Abdurahman, N. H., & Olalere, O. A. (2017). Journal of King Saud University – Science Ethanolic extraction of flavonoids , phenolics and antioxidants from Vernonia amygdalina leaf using two-level factorial design. *Journal of King Saud University - Science*, 1–10.

Alavijeh, P. K., Alavijeh, P. K., Sharma, D., & Pharmacy, C. (2012). A study of antimicrobial activity of few medicinal herbs, *2*(4), 496–502.

Atarod, M., Nasrollahzadeh, M., & Sajadi, S. M. (2016). Journal of Colloid and Interface Science Green synthesis of Pd / RGO / Fe 3 O 4 nanocomposite using Withania coagulans leaf extract and its application as magnetically separable and reusable catalyst for the reduction of 4-nitrophenol. *JOURNAL OF COLLOID AND INTERFACE SCIENCE*, *465*, 249–258.

Baba, S. A., & Malik, S. A. (2015). Determination of total phenolic and flavonoid content , antimicrobial and antioxidant activity of a root extract of Arisaema jacquemontii Blume. *Integrative Medicine Research*, *9*(4), 449–454.

Balamurugan, M., Saravanan, S., & Soga, T. (2014). Synthesis of Iron Oxide Nanoparticles by Using Eucalyptus Globulus Plant Extract. *E-Journal of Surface Science and Nanotechnology*, *12*(0), 363–367.

Chaki, S. H., Malek, T. J., Chaudhary, M. D., Tailor, J. P., & Deshpande, M. P. (n.d.). Magnetite Fe 3 O 4 nanoparticles synthesis by wet chemical reduction and their characterization.

Devatha, C. P., Jagadeesh, K., & Patil, M. (2018). Environmental Nanotechnology , Monitoring & Management E ff ect of Green synthesized iron nanoparticles by Azardirachta Indica in di ff erent proportions on antibacterial activity. *Environmental Nanotechnology, Monitoring & Management*, *9*(November 2017), 85–94.

Enrique, C., Castro, B., Saucedo-, E. M., Morales, R. M. C., Soto, D. I. R., Treviño, F. M., & Carrazco, J. L. (2018). In vivo antimicrobial activity of silver nanoparticles produced via a green chemistry

synthesis using Acacia rigidula as a reducing and capping agent, 2349–2363.

Fierascu, R. C., Bunghez, I. R., Somoghi, R., Fierascu, I., & Ion, R. M. (2014). Characterization of Silver Nanoparticles Obtained By Using Rosmarinus Officinalis Extract and their antioxidant activity. *Rev. Roum. Chim.*, *59*(March), 213–218.

Frieri, M., Kumar, K., & Boutin, A. (2017). Antibiotic resistance. *Journal of Infection and Public Health*, *10*(4), 369–378.

Ganesan, V. (2015). ECO-FRIENDLY SYNTHESIS AND CHARACTERIZATION OF SILVER NANOPARTICLES SYNTHESIZED AT DIFFERENT P H USING LEAF BROTH OF HYPTIS SUAVEOLENS (L .) POIT ECO-FRIENDLY SYNTHESIS AND CHARACTERIZATION OF SILVER NANOPARTICLES SYNTHESIZED AT DIFFERENT P H USING LEAF, (September).

Gondwal, M. (2018). Synthesis and Catalytic and Biological Activities of Silver and Copper Nanoparticles Using Cassia occidentalis, *2018*.

Groiss, S., Selvaraj, R., Varadavenkatesan, T., & Vinayagam, R. (2017). Structural characterization, antibacterial and catalytic effect of iron oxide nanoparticles synthesised using the leaf extract of Cynometra ramiflora. *Journal of Molecular Structure*, *1128*(September), 572–578.

Gupta, M., & Gupta, S. (2014). Qualitative and Quantitative Analysis of Phytochemicals and Pharmacological Value of Some Dye Yielding Medicinal Plants Qualitative and Quantitative Analysis of Phytochemicals and Pharmacological Value of Some, (May).

Heera, P., & Shanmugam, S. (2015). Review Article Nanoparticle Characterization and Application : An Overview, *4*(8), 379–386.

Hills, M., Khan, A. M., Qureshi, R. A., Gillani, S. A., & Ullah, F. (2014). Antimicrobial activity of selected medicinal plants of, (March 2011).

Jain, S., & Mehata, M. S. (2017). Medicinal Plant Leaf Extract and Pure Flavonoid Mediated Green Synthesis of Silver Nanoparticles and their Enhanced Antibacterial Property. *Scientific Reports*, *7*(1), 1–13.

Jing, L., Ma, H., Fan, P., Gao, R., & Jia, Z. (2015). Antioxidant potential, total phenolic and total flavonoid contents of Rhododendron anthopogonoides and its protective effect on hypoxia-induced injury in PC12 cells. *BMC Complementary and Alternative Medicine*, *15*(1), 1–12.

Joe, J., Sivalingam, P., Siva, D., Kamalakkannan, S., Anbarasu, K., Sukirtha, R., … Achiraman, S. (2011). Colloids and Surfaces B : Biointerfaces Comparative evaluation of antibacterial activity of silver nanoparticles synthesized using Rhizophora apiculata and glucose. *Colloids and Surfaces B: Biointerfaces*, *88*(1), 134–140.

Kanagasubbulakshmi, S., & Kadirvelu, K. (2017). Green Synthesis of Iron Oxide Nanoparticles using Lagenaria Siceraria and Evaluation of its Antimicrobial Activity, *2*(4), 422–427.

Khalid, S., Shahzad, A., Basharat, N., Abubakar, M., & Anwar, P. (2018). Phytochemical Screening and Analysis of Selected Medicinal Plants in Phytochemistry & Biochemistry, *2*(1), 2–4.

Khan, I., Saeed, K., & Khan, I. (2017). Nanoparticles : Properties , applications and toxicities. *Arabian Journal of Chemistry*.

Khodadadi, B., Bordbar, M., & Nasrollahzadeh, M. (2017). Journal of Colloid and Interface Science Achillea millefolium L . extract mediated green synthesis of waste peach kernel shell supported silver nanoparticles : Application of the nanoparticles for catalytic reduction of a variety of dyes in water. *Journal of Colloid And Interface Science*, *493*, 85–93.

Ksv, G., P, H. R., & Zamare, D. (2017). Biotherapeutic Discovery Green Synthesis of Iron Nanoparticles Using Green Tea leaves Extract, *7*(1), 1–4.

Kuppusamy, P., Yusoff, M. M., & Maniam, G. P. (2016). Biosynthesis of metallic nanoparticles using plant derivatives and their new avenues in pharmacological applications – An updated report. *Saudi Pharmaceutical Journal*, *24*(4), 473–484.

Leung, E., Weil, D. E., Raviglione, M., & Nakatani, H. (2011). The WHO policy package to combat antimicrobial resistance. *Bulletin of the World Health Organization*, *89*(5), 390–392.

Logeswari, P., Silambarasan, S., & Abraham, J. (2015). Synthesis of silver nanoparticles using plants extract and analysis of their antimicrobial property. *Journal of Saudi Chemical Society*, *19*(3), 311–317.

Madivoli, E. S., Maina, E. G., Kairigo, P. K., Murigi, M. K., Ogilo, J. K., Nyangau, J. O., … Madivoli, E. (2012). In vitro a ntioxidant and antimicrobial activity of Prunus africana (Hook . f .) Kalkman (bark extracts) and Harrisonia abyssinica Oliv . extracts (bark extracts): A comparative study, 1–9.

Makarov, V. V, Love, A. J., Sinitsyna, O. V, Makarova, S. S., & Yaminsky, I. V. (2014). " Green " Nanotechnologies : Synthesis of Metal Nanoparticles Using Plants, *6*(20), 35–44.

Marslin, G., Siram, K., Maqbool, Q., Selvakesavan, R. K., Kruszka, D., Kachlicki, P., & Franklin, G. (2018). Secondary metabolites in the green synthesis of metallic nanoparticles. *Materials*, *11*(6).

Martínez-cabanas, M., López-garcía, M., Barriada, J. L., Herrero, R., & Vicente, M. E. S. De. (2016). Green synthesis of iron oxide nanoparticles. Development of magnetic hybrid materials for efficient As (V) removal. *CHEMICAL ENGINEERING JOURNAL*, (V).

Mostafa, A. A., Al-askar, A. A., Almaary, K. S., Dawoud, T. M., Sholkamy, E. N., & Bakri, M. M. (2017). Antimicrobial activity of some plant extracts against bacterial strains causing food poisoning diseases. *Saudi Journal of Biological Sciences*.

Prabhavathi, R. M., Prasad, M. P., & Jayaramu, M. (2016). Studies on Qualitative and Quantitative Phytochemical Analysis of Cissus quadrangularis, *7*(4), 11–17.

Rafi, M., Id, S., Khan, M., Id, M. K., Al-warthan, A., Mahmood, A., … Adil, S. F. (n.d.). Plant-Extract-Assisted Green Synthesis of Silver Nanoparticles Using Origanum vulgare L . Extract and Their Microbicidal Activities, 1–14.

Ranjitha, S., & Suganthi, A. (2017). Preliminary phytochemical analysis of galinsoga parviflora (Cav) leaves and flowers, *2*(3), 18–20.

Samaneh, S., Nasrollahzadeh, M., & Rustaiyan, A. (2017). Journal of Colloid and Interface Science Biosynthesis and application of Ag / bone nanocomposite for the hydration of cyanamides in Myrica gale L . extract as a green solvent. *Journal of Colloid And Interface Science*, *499*, 93–101.

Santos, F. S. Dos, Lago, F. R., Yokoyama, L., & Fonseca, F. V. (2017). Synthesis and characterization of zero-valent iron nanoparticles supported on SBA-15. *Journal of Materials Research and Technology*, *6*(2), 178–183.

Saranya, S. (2017). Green Synthesis of Iron Nanoparticles using Aqueous Extract of Musa ornata Flower Sheath against Pathogenic Bacteria, *79*(January), 688–694.

Silveira, C., Shimabuku, Q. L., & Silva, M. F. (2017). Iron-oxide nanoparticles by the green synthesis method using Moringa oleifera leaf extract for fluoride removal, *3330*.

Spiridon, I., Bodirlau, R., & Teaca, C. (2011). Total phenolic content and antioxidant activity of plants used in traditional Romanian herbal medicine, *6*(3).

Ullah, A., Kareem, A., Nami, S. A. A., Shoeb, M., & Rehman, S. (2018). Journal of Photochemistry & Photobiology , B : Biology Biogenic synthesis of iron oxide nanoparticles using Agrewia optiva and Prunus persica phyto species : Characterization , antibacterial and antioxidant activity. *Journal of Photochemistry & Photobiology, B: Biology*, *185*(April), 262–274.

Vélez, E., Campillo, G., Morales, G., Hincapié, C., Osorio, J., & Arnache, O. (2018). Silver Nanoparticles Obtained by Aqueous or Ethanolic Aloe vera Extracts : An Assessment of the Antibacterial Activity and Mercury Removal Capability, *2018*.

Wang, Z., Fang, C., & Megharaj, M. (2014). Characterization of Iron − Polyphenol Nanoparticles Synthesized by Three Plant Extracts and Their Fenton Oxidation of Azo Dye, 10–13.

Wu, W., He, Q., & Jiang, C. (2008). Magnetic iron oxide nanoparticles: Synthesis and surface functionalization strategies. *Nanoscale Research Letters*, *3*(11), 397–415.

Xiao, J., Chen, G., & Li, N. (2018). Ionic Liquid Solutions as a Green Tool for the Extraction and Isolation of Natural Products. *MDPI*, 23.

Yuvakkumar, R., Elango, V., Rajendran, V., & Kannan, N. (2011). PREPARATION AND CHARACTERIZATION OF ZERO VALENT IRON, *6*(4), 1771–1776.